Journal of Biomedical Materials Research Part B: Applied Biomaterials

Cytocompatibility assessment of Ti-Zr-Pd-Si-(Nb) alloys with low Young's modulus, increased hardness and enhanced osteoblast differentiation for biomedical applications

Journal:	*Journal of Biomedical Materials Research: Part B - Applied Biomaterials*
Manuscript ID	JBMR-B-16-0419.R2
Wiley - Manuscript type:	Original Research Report
Date Submitted by the Author:	n/a
Complete List of Authors:	Blanquer, Andreu; Universitat Autonoma de Barcelona, Biologia Cel·lular, Fisiologia i Immunologia Musilkova, Jana; Institute of Physiology, Academy of Sciences of the Czech Republic, Prague, Growth and Differentiation of Cell Populations Barrios, Leonardo; Universitat Autonoma de Barcelona, Departament de Biologia Cel·lular, Fisiologia i Immunologia Ibáñez, Elena; Universitat Autonoma de Barcelona, Departament de Biologia Cel·lular, Fisiologia i Immunologia Vandrovcova, Marta; Academy of Sciences of the Czech Republic, Institute of Physiology Pellicer, Eva; Universitat Autonoma de Barcelona, Física de Materials II Sort, Jordi; Institució Catalana de Recerca i Estudis Avançats (ICREA) , - Bačáková, Lucie; Institute of Physiology, Academy of Sciences of the Czech Republic, Prague, Growth and Differentiation of Cell Populations Nogués, Carme; Universitat Autonoma de Barcelona, Departament de Biologia Cel·lular, Fisiologia i Immunologia
Keywords:	Ti-based alloy, Saos-2 cells, osteogenic genes expression, protein adsorption, cytocompatibility

Submitted version. The published version is available at DOi 10.1002/jbm.b.33892

Cytocompatibility assessment of Ti-Zr-Pd-Si-(Nb) alloys with low Young's modulus, increased hardness and enhanced osteoblast differentiation for biomedical applications

Andreu Blanquer[1], Jana Musilkova[2], Leonardo Barrios[1], Elena Ibáñez[1], Marta Vandrovcova[2], Eva Pellicer[3], Jordi Sort[4], Lucie Bacakova[2], Carme Nogués[1]

[1]*Departament de Biologia Cel·lular, Fisiologia i Immunologia, Universitat Autònoma de Barcelona, E-08193 Bellaterra, Spain*

[2]*Institute of Physiology, Academy of Sciences of the Czech Republic, 14220 Prague 4 Czech Republic*

[3]*Departament de Física, Universitat Autònoma de Barcelona, E-08193 Bellaterra, Spain*

[4]*Institució Catalana de Recerca i Estudis Avançats (ICREA) and Departament de Física, Universitat Autònoma de Barcelona, E-08193 Bellaterra, Spain*

**Corresponding author. E-mail address: carme.nogues@uab.cat*

Abstract

Ti-based alloys have increased importance for biomedical applications due to their excellent properties. In particular, the two recently developed TiZrPdSi(Nb) alloys, with a predominant β-Ti phase microstructure, have good mechanical properties, such as a relatively low Young's modulus and high hardness. In the present work, the cytocompatibility of these alloys was assessed using human osteoblast-like Saos-2 cells. Cells grown on the alloys showed larger spreading areas (more than twice) and higher vinculin content (nearly 40% increment) when compared with cells grown on glass control surfaces, indicating a better cell adhesion. Moreover, cell proliferation was 18% higher for cells growing on both alloys than for cells growing on glass and polystyrene control surfaces. Osteogenic differentiation was evaluated by quantifying the expression of four osteogenic genes (osteonectin, osteocalcin, osteopontin and bone sialoprotein), the presence of three osteogenic proteins (alkaline phosphatase, collagen I and osteocalcin) and the activity of alkaline phosphatase at different time-points. The results demonstrated that TiZrPdSi and TiZrPdSiNb alloys enhance osteoblast differentiation, and that cells grown on TiZrPdSiNb alloy present higher levels of some late osteogenic markers during the first week in culture. These results suggest that the TiZrPdSi(Nb) alloys can be considered as excellent candidates for orthopaedical uses.

Keywords: Ti-based alloy, protein adsorption, Saos-2 cells, cytocompatibility, osteogenic gene expression

Running title: Ti-Zr-Pd-Si-(Nb) alloys for biomedical applications

1. Introduction

Titanium-based alloys have attracted much attention in the orthopedic field for long-term bone implants because of their better physico-chemical and mechanical properties compared with other metallic alloys and biocompatible materials. Different Ti-based alloys, with different combinations of non-toxic elements, are being investigated in order to improve their properties, including elasticity and hardness. Suitable elastic properties, meaning a not exceedingly high Young's modulus, are among the key factors to be taken into account when evaluating the potential use of an alloy in bone implants. Alloys with a Young's modulus close to that of the cortical bone (20-30 GPa) tend to be more suitable for orthopedic applications, as this reduces the "stress shielding effect", a biomechanical incompatibility that can result in implant loosening [(1)]. Hardness is also an important property, and current efforts are focused on trying to synthesize new alloys with reduced Young´s moduli, while maintaining or increasing their hardness. Nowadays, one of the most used Ti-based alloys is the commercially available Ti-6Al-4V, with a hardness of 5 GPa and a Young's modulus of 110 GPa, which is much higher than that of the cortical bone. Thus, new Ti-based alloys with higher elasticity (lower Young's modulus) and hardness, but maintaining other good properties such as low corrosion and wear resistance, are under development.

The physical, chemical and mechanical properties of an alloy can be readily modified by changing its composition (elements and percentage). But, because some elements have been described as cytotoxic, they should not be used for the synthesis of alloys for biomedical applications. The cytotoxicity of the most commonly used elements in implant alloys has been studied by many researchers and, in 2012, Biesiekierski et al. published an extensive review on the biocompatibility, carcinogenicity, genotoxicity, mutagenicity, cytotoxicity, allergenicity and the proneness to corrosion of 27 transition metals [(2)]. In that study, Vanadium, Beryllium, Cadmium and Cobalt are described as cytotoxic elements. Aluminum is known to have adverse effects and it seems to be involved in severe neurological diseases and to play a role in neurodegeneration [(3),(4)]. All authors agree on the allergenic effect of Nickel [(5),(6)], and some of them also consider Nickel ions to be cytotoxic and to have a potential carcinogenic effect. On the other hand,

Titanium, Zirconium, Tantalum, Niobium and Palladium are considered as low cytotoxic elements and, thus, they can be safely used to synthesize biocompatible medical alloys [7].

Regarding alloy biocompatibility, osseointegration is an important issue, and thus the interactions between cells and the alloy surface should be carefully analyzed. Topography, wettability and surface charge are parameters that can modulate cell response. In general, cell adhesion increases with surface hydrophilicity, and it is mediated through the recognition and adhesion to extracellular matrix molecules (collagen, fibronectin, laminin, etc.). Proteins from the serum are adsorbed onto alloy surfaces, facilitating the contact with the cell membrane receptors. Fibronectin, collagen and laminin are considered promoters of cell adhesion whereas proteins like albumin are considered inhibitors of cell adhesion. Thus, cell adhesion can be modulated depending on the affinity of different types of proteins for the alloy surface. Adhesion is mandatory for all anchorage-dependent cells, like osteoblasts, to resume the cell cycle and hence to allow cell proliferation [8]. Osteoblast adhesion to the implant material and consequent spreading is mediated by integrins, a family of adhesion proteins that act as receptors for the extracellular matrix proteins collagen, laminin or fibronectin. When integrins contact fibronectins, they cluster and trigger the formation of focal contacts together with other cytosolic proteins such as talin, vinculin and paxillin.

Adhesion, however, is not the only biological property that a biomaterial must permit. It should also allow osteoblast differentiation, that is, cells should be allowed to synthesize the proteins needed to produce and mineralize the extracellular matrix. Osteoblast differentiation in the bone is a continuous process that can be divided in three different stages: i) proliferation, ii) osteogenic proteins expression and secretion, and iii) mineralization of extracellular matrix [9]. During the osteogenic protein expression stage, several proteins can be detected *in vitro* at different time-points. For example, collagen I (COLI) and alkaline phosphatase (ALP) activity are considered early osteogenic markers, whereas osteocalcin (OC), bone sialoprotein (BSP), osteopontin (OPN) and osteonectin (ON) are considered late osteogenic markers. The study of the expression of specific osteogenic genes, and the detection of specific proteins at different time-points is therefore important to determine whether the alloy affects the differentiation patterns.

The microstructure, mechanical properties and short-term biological response of the TiZrPdSi(Nb) alloy were studied in a previous work by our group [10]. Microstructure consisted of a predominant β-Ti phase and additional phases in smaller volume fractions. In terms of mechanical properties, the $Ti_{45}Zr_{15}Pd_{30}Si_5Nb_5$ alloy exhibited lower Young's modulus and hardness (85 GPa and 10.4 GPa, respectively) than the $Ti_{45}Zr_{15}Pd_{35}Si_5$ alloy (117 GPa and 14.2 GPa, respectively). Moreover, preliminary short-term biological tests at 24 h indicated high cell viability and complete osteoblast adhesion on both alloy surfaces. These previous results suggested that these alloys possess a great potential to be used as permanent implants for bone repair purposes.

Due to the great potential of these two metallic alloys ($Ti_{45}Zr_{15}Pd_{35}Si_5$ and $Ti_{45}Zr_{15}Pd_{30}Si_5Nb_5$), in the present study we aimed to compare the effect of Nb addition by deepening on the cytocompatibility analysis by performing short- and medium-term studies. First, we evaluated the capacity of both alloys to adsorb two proteins present in the serum: albumin and fibronectin. Second, we quantified the initial adhesion response (cell spreading and vinculin quantification), proliferation over 7 days in culture and osteogenic differentiation of human osteoblast-like Saos-2 cells growing on both alloys and on control surfaces. Third, we quantified the expression of four osteogenic genes (ON, OC, BSP and OPN), the presence of three osteogenic proteins (ALP, COL I and OC) and the activity of ALP at different time-points to determine whether cell differentiation on both alloys followed the expected pattern.

2. Material and Methods

2.1. Alloy samples

Master alloys with composition $Ti_{45}Zr_{15}Pd_{35-x}Si_5Nb_x$ (where x=0 and 5 at. %) were prepared by arc melting a mixture of the highly pure elements (>99.99% wt %) under a Ti-gettered Ar atmosphere on a water-cooled Cu heart. Rods of 3 mm in diameter were obtained from the melt by suction casting into a Cu mould. Disks of approximately 500 µm in thickness were cut from the rods, and carefully grinded with SiC paper (up to 4,000 grit) to obtain a mirror glass surface, degreased with acetone and finally cleaned with distilled water in an ultrasonic bath. For the following experiments, 42 disks were prepared for each alloy composition.

From now on, we will refer to $Ti_{45}Zr_{15}Pd_{35}Si_5$ as TiZrPdSi and to $Ti_{45}Zr_{15}Pd_{30}Si_5Nb_5$ as TiZrPdSiNb.

2.2. Contact angle measurements

To assess the wettability of the alloy surfaces, the contact angle of an aqueous drop (1.5 µl) of McCoy's culture medium (Sigma-Aldrich, St. Louis, MO, USA) supplemented with 10% fetal bovine serum (FBS; Sigma-Aldrich, St. Louis, MO, USA) and deposited onto the surface of the alloy was measured using a Contact Angle Measuring System DSA 100 (Krüss, Haburg, Germany) at room temperature (RT). Three different disks were analyzed for each composition. The glass coverslip surface was used as a control.

2.3. Quantification of protein adsorption

To quantify the amount of protein adsorbed on the surface of the alloy, samples were submerged overnight at 4°C in a phosphate buffered solution (PBS; Sigma-Aldrich, St. Louis, MO, USA) containing 5 µg/ml of bovine serum albumin (Sigma-Aldrich, St. Louis, MO, USA) or fibronectin (Roche Diagnostics, Basel, Switzerland). After incubation, samples were washed thrice with PBS and non-specific binding sites were blocked by 1% Tween (Sigma-Aldrich, St. Louis, MO, USA) in PBS for 20 min at room temperature (RT). Then, samples were incubated with anti-albumin (Sigma-Aldrich, St. Louis, MO, USA) or anti-fibronectin (Sigma-Aldrich, St. Louis, MO, USA) antibodies (1:200) at RT for 1 h, washed thrice with PBS and incubated with HRP peroxidase-conjugated secondary antibody (1:1000) (Sigma-Aldrich, St. Louis, MO, USA) at RT for 1 h. Afterwards, samples were washed four times with PBS and transferred to a new plate where they were incubated for 20 min at RT in agitation in a 2,2'-azino-bis(3-ethylbenzothiazoline-6-sulfonic acid) (ABTS) solution (0.1M NaOAc; 0.05 NaH_2PO_4; 21.9 mg/ml ABTS (Sigma-Aldrich, St. Louis, MO, USA) in ddH_2O at pH 5) and 30% H_2O_2. Finally, supernatants were transferred to an ELISA plate and read with a spectrophotometer at 405 nm (Synergy HT, BioTek, Winooski, VT, USA). Experiments were performed in triplicate for each alloy using a different disk each time, and for each negative control without primary antibody.

2.4. Cell culture

Alloy disks were sterilized with absolute ethanol for 2 h and individually inserted into 24-well cell culture plates. A total of 50,000 Saos-2 cells (European Collection of Cell Cultures, Salisbury, UK) were seeded and cultured in McCoy's 5A medium supplemented with 10% FBS (Sigma-Aldrich, St. Louis, MO, USA) and 40 µg/ml gentamicin (LEK, Ljubljana, Slovenia) under standard conditions (37°C and 5% CO_2). Cells grown directly on standard tissue culture polystyrene wells and on glass coverslips, specific for cell cultures, were used as controls, because are optimum material for cell adhesion and growth.

2.5. Spreading area measurement

The spreading area of the cells adhered onto the alloy (with or without Nb) and control (polystyrene and glass) surfaces was quantified after 24 h of seeding. Cells were rinsed with PBS, fixed with frozen 70% ethanol at RT for 20 min, and stained with a combination of the cell membrane dye Texas Red C_2-maleimide (Thermo Fisher Scientific, Waltham, MA, USA) and the nuclear dye Hoechst 33258 (Sigma-Aldrich, St. Louis, MO, USA) at RT for 1 h. Microphotographs of adhered cells were captured under an IX-50 microscope equipped with a DP 70 digital camera (both from Olympus, Tokyo, Japan). The spreading area of each individual cell (a minimum of 215 cells/sample) was measured using the Atlas software (Tescan, Brno, Czech Republic). Cells with intercellular contacts were excluded from the evaluation. Four independent experiments using different disks (n=4) were analyzed for each alloy tested and for controls.

2.6. Vinculin immunodetection and actin staining

The presence of focal adhesion plaques by vinculin immunodetection was quantified after 3 days of cells growing on top of the alloys and glass coverslips. Cells were rinsed twice in PBS, fixed with frozen 70% ethanol for 20 min, incubated with 1% bovine serum albumin (BSA) in PBS containing 0.05% Triton X-100 (Sigma-Aldrich, St. Louis, MO, USA) for 20 min at RT, and treated with 1% Tween for 20 min. Then, cells were incubated with a mouse monoclonal anti-human vinculin primary antibody (Sigma-Aldrich, St. Louis, MO, USA) at 4°C overnight. After rinsing twice in PBS, goat anti-mouse IgG secondary antibody conjugated with Alexa Fluor 488 (Thermo Fisher Scientific, Waltham, MA, USA) was applied for 1 h at RT simultaneously with the nuclear dye Hoechst 33258 and phalloidin conjugated with TRITC (1:1000, Sigma-Aldrich, St. Louis,

MO, USA). Images of different regions of the samples were taken under both an IX-50 inverted fluorescence microscope (Olympus, Tokyo, Japan) and a laser scanning confocal microscope (Leica TCS SP2, Wetzlar, Germany). To measure the fluorescence intensity, 8 micrographs from each sample were taken with the same exposure time and analyzed using Fluorescence Image Analyser software (ver. 1.1, 2013, available from http://alice.fbmi.cvut.cz/software/fia). A single color plane threshold was set on each image to remove the non-protein area from the image data. The same threshold and color plane settings were used for all images. Then the cumulative sum of all pixel intensities was evaluated and the background intensity of the negative staining control was subtracted. The total immunofluorescence intensity of the protein was normalized to the pixels evaluated. Three independent experiments (n= 3) using different disks were used for each composition and control.

2.7. Quantification of cell proliferation

Cell proliferation on metallic alloys and control surfaces was quantified by counting the number of cells at different time-points. After 1, 3 and 7 days of cell seeding, cells were stained with the nuclear dye Hoechst 33258, and randomly selected fields were photographed in order to quantify the number of nuclei (cells) on each sample. Three independent experiments were performed using different disks (n= 3).

2.8. Quantitative real-time PCR (qPCR)

The qPCR was performed to determine the expression profile of four osteoblast genes expression. Saos-2 cells were grown for 7 and 14 days on the alloy and glass (control) surfaces. Total RNA was extracted from the cell cultures using Total RNA purification micro kit (Norgen Biotek, Thorold, ON, Canada) according to the manufacturer's protocol. The RNA concentration was measured using the NanoPhotometer (Implen, Munich, Germany). Reverse transcription was performed on 100 ng of total RNA using the ProtoScript M-MuLV First Strand cDNA synthesis kit (New England BioLabs, Ipswich, MA, USA) according to manufacturer's protocol using a T Personal Thermocycler (Biometra, Göttingen, Germany). The mRNA levels were quantified using quantitative real time 5xHOT FIREPol Probe qPCR Mix Plus (ROX) (Solis BioDyne, Tartu, Estonia) and with TaqMan Gene Expression Assays (Thermo Fischer Scientific, Waltham, MA, USA) labeled

with FAM reporter dye specific for human osteocalcin (OC; Hs01587814_g1), osteonectin (ON; Hs00234160_m1), osteopontin (OPN; Hs00959010_m1), bone sialoprotein (BSP; Hs00173720_m1) as target genes, and glyceraldehyde 3-phosphate dehydrogenase (GAPDH; Hs02758991_g1) as a reference gene, in final reaction volume of 20 μl per well on a 96-well optical reaction plate using the ViiaTM 7 Real-time PCR System. Data are the mean of 4–5 experimental points from 2 independent experiments. Expression values were obtained from Ct numbers. The target gene levels are expressed as a relative value, the ratio of the target gene expression towards the reference ACTB gene. The relative gene expression was calculated as $2^{-\Delta Ct}$. Three independent experiments using different disks (n= 3) were used for each composition and control.

2.9. Osteogenic markers immunodetection

Quantification of osteogenic markers was performed by immunodetection of three different proteins involved in osteoblast differentiation: COL I, OC and ALP. Saos-2 cells were cultured during 7 days onto alloys and control glass coverslips. Cells were then fixed in 4% paraformaldehyde in PBS for 30 min at RT, permeabilized with 1% BSA in PBS containing 0.05% Triton X-100 for 20 min, and treated with 1% Tween for 20 min at RT. Samples were then incubated overnight at 4ºC with primary antibodies: rabbit anti-osteocalcin (1:200; Peninsula Laboratories, San Carlos, CA, USA), mouse monoclonal anti-collagen I (1:200; Sigma-Aldrich, St. Louis, MO, USA) or mouse anti-ALP (Sigma-Aldrich, St. Louis, MO, USA). After being rinsed twice with PBS, cells were incubated for 1 h at RT with the secondary antibody Alexa Fluor 488-conjugated goat anti-rabbit (Thermo Fisher Scientific, Waltham, MA, USA) or Alexa Fluor 488-conjugated goat anti-mouse (Thermo Fisher Scientific, Waltham, MA, USA) diluted 1:400 in PBS together with the nuclear dye Hoechst 33258. Images from randomly selected regions were captured and fluorescence intensity was measured as previously described for vinculin immunodetection. Three independent experiments using different disks (n= 3) were used for each composition and control.

2.10. Quantification of ALP activity

Saos-2 cells differentiation on alloys and control surfaces was also studied measuring the ALP activity. Cells were cultured onto the samples during 7 and 14 days. Each sample was transferred to an Eppendorf tube and cells were lysed for 10 min in CyQuant cell lysis buffer (Thermo Fisher Scientific, Waltham, MA, USA) and then vortexed for 10 sec. Cell lysates were centrifuged at 12,000 rpm for 4 min at 4°C, and supernatants were collected. ALP activity was determined by the hydrolysis of p-nitrophenyl phosphate (pNPP), which produces p-nitrophenol (pNP). Briefly, 25 µl of 1-step pNPP (Thermo Fisher Scientific, Waltham, MA, USA) was added to 25 µl of supernatant. After 30 min incubation at RT, 2 M NaOH was added to stop the reaction. The absorbance was measured at 405 nm using a spectrophotometer. ALP activity was normalized to total protein content using Micro BCA Protein Assay kit (Thermo Fisher Scientific, Waltham, MA, USA), according to the manufacturer's protocol. Three independent experiments using different disks (n= 3) were used for each alloy composition and control.

2.11. Statistical analysis

The quantitative data is presented as mean ± SD (Standard Deviation). Statistical comparisons were performed using one-way analysis of variance (ANOVA) with Tukey-Kramer multiple comparison test for protein immunodetection and cell proliferation assays. The Kruskal-Wallis test with Dunn's multiple comparisons was used for protein adsorption, spreading area and ALP activity assays. Multiple comparison procedures were performed with ANOVA using the Student-Newman-Keuls method for gene expression values. In all cases, the analysis was performed using GraphPad Prism (GraphPad software, La Jolla, CA, USA) and a value of $p<0.05$ was considered statistically significant.

Significance is represented in the figures using an alphabetical superscript system on top of the columns. Letters shared in common between or among the groups indicate no significant differences whereas different letters indicate statistically significant differences.

3. Results

3.1. Wettability

The contact angle values were 57.6± 6.5 ° for the TiZrPdSi alloy and 64.8± 4.7 ° for the TiZrPdSiNb alloy, both slightly lower than the value for the glass coverslip used as control (80.0 ± 1.0 °).

3.2. Albumin and fibronectin adsorption

Albumin was significantly more adsorbed on the TiZrPdSiNb alloy surface than in TiZrPdSi and control surfaces (Fig. 1a). The amount of protein adsorbed was similar on TiZrPdSi and glass surfaces, and significantly lower in polystyrene surface. A similar tendency was observed for fibronectin (Fig. 1b), with a significantly increased adsorption on TiZrPdSiNb surface.

3.3. Cell spreading

Individual cell spreading areas of Saos-2 cells grown on tested alloys and controls were measured after 24 h. Osteoblasts adhered on all surfaces tested and no significant differences were found between cells growing on the two alloy compositions tested (TiZrPdSi: 784 ± 27 and TiZrPdSiNb: 734 ± 27 μm^2), and the polystyrene control (739 ± 31 μm^2). However, a significantly reduced spreading area was observed on cells grown on the glass coverslip (352 ± 15 μm^2) (Fig. 2).

3.4. Cell adhesion and vinculin immunodetection

Immunofluorescence detection of vinculin, a protein involved in focal contacts, and staining of actin filaments, the constituents of stress fibers, was next performed in order to further investigate osteoblasts adhesion on the sample surfaces. After 3 days in culture, Saos-2 cells presented diffuse free vinculin in the cytoplasm and defined spots of vinculin integrated in focal adhesion plaques that co-localized at the cell periphery with the ends of the stress fibers on all surfaces tested (Fig. 3). Well-defined stress fibers, some of them crossing the cell from end to end, were observed in all cases. Moreover, images of vinculin immunodetection were used to quantify the fluorescence intensity. Results indicated no significant differences in fluorescence intensity between the two alloys tested, but both showed significantly higher intensities than the glass coverslip control (Fig. 3d).

3.5. Cell proliferation

The proliferation of Saos-2 cells grown on the two alloys was quantified at days 1, 3 and 7 and compared with the proliferation on control samples (glass and PS). As it can be seen in figure 4, the number of cells growing on both alloys was significantly higher than the cells growing on both controls after 1 day in culture. The same tendency was observed after 3 and 7 days. On the other hand, no significant differences in cell proliferation were observed between the two alloyed compositions, or between both controls.

3.6. Expression of osteogenic markers

The expression of four specific osteoblast differentiation markers (OC, OPN, ON, BSP) was evaluated after 7 and 14 days in culture on both alloys and on glass surfaces. The level of OC mRNA after 7 days was nearly twice in TiZrPdSiNb compared with the level in TiZrPdSi and glass. However, after 14 days, the level of OC mRNA was similar in cells growing on both alloys, and significantly higher than in cells growing on the glass coverslip. Expression of OPN was similar to that of OC at 7 days, but at 14 days of culture it was significantly lower in cells grown on TiZrPdSiNb than on the TiZrPdSi alloy. Differences in ON mRNA levels were detected only between TiZrPdSi and glass at 7 days in culture. Finally, the expression of BSP was similar for both alloys, and significant lower for the glass control at 7 days of culture. However, the situation was reversed at 14 days of culture, being BSP expression significantly higher in cells growing on glass than on both alloys.

3.7. Osteogenic proteins

Osteoblast differentiation was also evaluated by quantifying the immunodetection of COLI, OC and ALP after 7 days in culture. No significant differences in COLI levels were found between the two alloys tested, but a significantly smaller amount of this protein was detected in cells grown on the glass coverslip (Fig. 6a). Cells grown on TiZrPdSiNb presented a larger amount of OC (117 a.u.) than on TiZrPdSi (77 a.u.) and glass coverslip (60 a.u) (Fig. 6b). Finally, TiZrPdSi alloy showed the largest amount of ALP protein (Fig. 6c).

3.8. ALP activity

ALP activity is also a marker for osteoblast differentiation. After 7 days, no significant differences were observed among the two alloys tested and the control glass surfaces (Fig. 7). However, after 14 days, ALP activity had strongly increased in both alloys, but decreased on cells grown on glass coverslips.

4. Discussion

Nanostructured TiZrPdSi(Nb) alloys were previously characterized by our group and showed a good combination of elasticity (TiZrPdSiNb 85 GPa; TiZrPdSi 117 GPa) and hardness (TiZrPdSiNb 10.4 GPa; TiZrPdSi 14.2 GPa), better than the commercially available Ti-6Al-4V and Ti-40Nb alloys [10]. The addition of Nb to the alloy (TiZrPdSiNb) resulted in a lower Young's modulus, closer to that of the bone, but also in a lower hardness than its counterpart (TiZrPdSi). Importantly, we also demonstrated that the addition of Nb to the alloy did not produce cytotoxicity nor affected cell adhesion at 24 h of culture. Altogether, the results of this previous work suggested that TiZrPdSi(Nb) is a promising candidate to be used in bone implants. However, further analyses of cytocompatibility were necessary to demonstrate its safeness in short- and medium-term biological conditions. Wettability and topography of the alloy are important characteristics for cell adhesion and growth. In general, osteoblast adhesion and spreading improves with an increase in surface hydrophilicity, measured by the contact angle [11]. Protein adsorption is the first biological event that occurs when a biomaterial is immersed in a medium supplemented with serum, and it depends on hydrophobic interactions. *In vitro* studies have shown that hydrophilic surfaces are able to adsorb proteins in a more flexible conformation than hydrophobic ones, and this flexibility allows their reorganization and improves cell adhesion and spreading [11]. Other factors like pH, surface charge and roughness are also important for protein adsorption. In the present study, we minimized the effect of topography by using mirror-like surface disks for both alloy compositions. Regarding wettability, contact angle results indicated that the TiZrPdSi alloy was slightly more hydrophilic than the TiZrPdSiNb alloy. It is known that cell adhesion is mediated through the ECM molecules adsorbed on the alloy surface, which increases with surface hydrophilicity. Moreover, cell adhesion depends on the type and concentration of the adsorbed proteins. Some authors have suggested that fibronectin promotes cell adhesion, whereas albumin prevents it [12].

Here, we show that TiZrPdSiNb adsorbed more albumin and fibronectin than the TiZrPdSi alloy, glass and PS, which could be related to its higher hydrophilicity, although it has been described that contact angles higher than 30° do not seem to affect fibronectin adsorption [13].

Saos-2 cells are osteosarcoma cells commonly used for biocompatibility studies due to their similarities with primary osteoblasts, including ALP activity and gene regulation upon differentiation [14]. Saos-2 cells are anchorage-dependent cells that need to adhere to survive and avoid the induction of anoikis, a type of regulated cell death unleashed when cells cannot adhere. Cell adhesion is mediated by integrins, a family of membrane receptors that bind to the extracellular ligands like fibronectin, collagen and laminin and that cluster to form focal adhesion plaques together with intracellular proteins such as vinculin. We found that, even though the alloy containing Nb (TiZrPdSiNb) adsorbed more fibronectin than the one lacking Nb, vinculin signal intensity was similar in cells grown on top of both alloys, suggesting an equivalent degree of cell adhesion to the alloy surface. A possible explanation is that although fibronectin and albumin are components of the serum, they compete to be adsorbed on the same surface and the increase in fibronectin adsorption is balanced by the increase in albumin adsorption. Moreover, the protein conformation once adsorbed to the surface of both alloys is unknown, and it is a key point in the subsequent cell response [15].

On the other hand, cell adhesion and spreading was lower on the glass coverslip, where more rounded cells were observed and lower levels of vinculin were quantified compared with both alloys. The higher contact angle of the glass coverslip (80 °) compared with that of the two alloys (57.6 ° and 64.8 °) can explain the differences in cell adhesion and spreading between the two different surfaces. These results are in agreement with those of other authors showing that contact angles of 60 ° or 64 ° allowed optimal cell adhesion and spreading compared to 90 ° [16]. Direct osteoblast adhesion and spreading on metal surfaces is important to prevent aseptic loosening of metal implants caused by fibroblast layer attachment and, for this reason, successful implant integration is highly dependent on the correct osteoblast adhesion on implant surface [17]. As cell adhesion was higher on both alloys, it is not surprising that cell proliferation was

also better on the alloys than on the controls, because Saos-2 cells cannot divide without previous adhesion [11].

Finally, the last item we analyzed was the ability of Saos-2 cells to differentiate onto the alloys. Osteoblast differentiation and extracellular matrix mineralization play an important role in osseointegration. OC, OPN, ON and BSP are osteogenic genes expressed by Saos-2 cells during the extracellular matrix maturation and mineralization [15],[18]. COLI is the major component of organic bone extracellular matrix, representing 90% of extracellular matrix proteins, and it is considered an early marker of osteoblast differentiation [19]. Another important marker in osteoblast differentiation is the ALP enzyme, which activity is necessary for extracellular matrix mineralization and reaches its maximum during early stages of differentiation [9]. We studied osteoblast differentiation at three different levels, first by quantifying the expression of four genes (OC, OPN, ON and BSP) at 7 and 14 days of culture; second, by detecting and quantifying three proteins (COLI, OC and ALP) at 7 days of culture; and third, by quantifying the activity of a protein (ALP) at 7 and 14 days of culture. In global, we can summarize that expression, presence and activity of the proteins analyzed in cells cultured during 7 days, were similar or higher on the alloys than on glass coverslip, except for ON. Between both alloys, differentiation seemed to be higher in the alloy containing Nb, according to the results of OC and OPN expression and of OC protein detection. At 14 days, the differences between alloys and glass were minimum in terms of gene expression, except for a still higher OC expression in both alloys, but ALP activity was still much higher in cells grown on the alloys than on glass coverslips. Thus, TiZrPdSi(Nb) alloys allowed a better osteoblast differentiation than glass coverslip. Moreover, the addition of Nb to the alloy increased both its cytocompatibility and its mechanical properties.

These results are in agreement with the good biological response that has been described for β-Ti alloys [20], the same microstructure present in TiZrPdSi and TiZrPdSiNb alloys. Guo et al. (2013) developed another β-Ti alloy, Ti-35Nb-2Ta-3Zr, and demonstrated, in *in vitro* studies, that the alloy enhanced cell proliferation and osteoblast differentiation in comparison with Ti-6Al-4V alloy, i.e. a material currently used for construction of clinically applied bone implants. In addition, our earlier study, also performed on β-Ti alloys,

showed that the adhesion and proliferation of human osteoblast-like U-2 OS cells and primary human osteoblasts on Ti–35Nb–7Zr–6Ta (TNZT) with various small additions of Fe and Si (particularly those with 0.5 wt.% of Si+ 2 wt.% of Fe) were higher than on the Ti-6Al-4V alloy. At the same time, the number of U-2 OS cells on Ti-6Al-4V was significantly lower than in control tissue culture polystyrene wells (by about 25%), and the number of human osteoblasts on Ti-6Al-4V was even ~8.5 times lower than on polystyrene wells [21]. The TNZT alloys also better promoted the production of collagen I, i.e. an early marker of osteogenic differentiation, in primary human osteoblasts than the Ti-6Al-4V alloy and standard cell culture polystyrene dishes [21]. Similar result were obtained in mouse osteoblast progenitor MC3T3-E1 cells, which proliferated more slowly on Ti-6Al-4V than on polystyrene, and on day 5 after seeding, they attained significantly lower cell population density (by about 30%) than on polystyrene. Also the amount of inorganic phosphate released by the mineralizing layers was markedly lower (more than 10 times) in MC3T3-E1 cells on Ti-6Al-4V than on tissue culture polystyrene on day 20 after seeding [22]. Coating Ti-6Al-4V alloy with bioactive glass increased the cell number above the value obtained on polystyrene, but the release of inorganic phosphate still remained significantly lower than on polystyrene [22]. In a study by Gittens *et al.* (2014), performed on primary human osteoblasts, the expression of certain markers of osteogenic cell differentiation, namely osteocalcin, bone morphogenetic proteins 2 and 4, gremlin 1 and noggin, and the expression of some subunits of integrin adhesion receptors, i.e α1, α2, β1 and β3, was similar on a smooth Ti6Al4V alloy and polystyrene dishes [23]. The expression of these markers on Ti-6Al-4V above the level obtained on polystyrene required roughening the Ti-6Al-4V surface, particularly creation of micrometer-scale roughness (Sa = 2.20 ± 0.42 μm) or combined micro-nanorougness (Sa = 2.08 ± 0.27 μm). However, in a study by Schwartz *et al.* (2008), roughening of Ti-6Al-4V surfaces (Ra from 0.2 μm to 3.3 μm decreased the number of human osteoblast-like MG63 cells and their activity of alkaline phosphatase under the levels obtained on polystyrene [24]. As for the glass coverslips, i.e. another reference material used in our study, this material supported the adhesion and growth of human fetal osteoblasts (hFOB 1.19) to a similar extent as Ti-6Al-4V, but the activity of alkaline phosphatase was markedly lower in cells on Ti-6Al-4V. This activity was improved by treatment of Ti-6Al-4V by micro arc oxidation [25]. From this point of view, the alloys newly

developed in the present study, seem to be more advantageous that Ti-6Al-4V, because the cell performance on these materials was in many parameters better or at least similar in comparison with polystyrene or glass controls without need of additional surface modifications of these materials.

Also on pure Ti, a standard clinically used material for bone implantation, particularly in stomatological surgery, the proliferation of human osteoblast-like cells of the Saos-2 and MG-63 lines was lower than on a TiNb alloy. At the same time, the cell growth on the TiNb alloy was significantly higher than on control cell culture polystyrene dishes, while on Ti, this number was similar or even lower in comparison with PS [15],[20]. Thus, it seems that the presence of β-Ti phase in an alloy is excellent to obtain biocompatible materials.

5. Conclusion

In conclusion, the TiZrPdSi(Nb) alloy system, with excellent mechanical properties, enhanced Saos-2 cells adhesion, spreading and proliferation in comparison with control tissue culture polystyrene wells and microscopic glass coverslips. Using three different methodologies we analyzed osteoblast differentiation, obtaining concordant results that demonstrated that TiZrPdSi and TiZrPdSiNb alloys allow a better osteoblast differentiation than control glass coverslips. Furthermore, our results showed that cells grown onto the TiZrPdSiNb alloy presented higher levels of some late osteogenic markers during the first week in culture. Thus, TiZrPdSi and TiZrPdSiNb alloys can be considered as excellent candidates to be used in orthopedical implants.

6. Acknowledgements

The study was supported by the Grant Agency of the Czech Republic (GACR, grant No. 15-01558S), the Spanish Ministerio de Ciencia e Innovación (MAT2014-57960-C03-1-R – co-financed by the Fondo Europeo de Desarrollo Regional, FEDER, and MAT2014-57960-C03-3-R projects), and the Generalitat de Catalunya (2014-SGR-524 and 2014-SGR-1015). AB was supported by a predoctoral grant from the Universitat Autònoma de Barcelona.

7. References

1. Geetha M, Singh AK, Asokamani R, Gogia AK. Ti based biomaterials, the ultimate choice for orthopaedic implants – A review. Prog Mater Sci 2009;54:397–425.

2. Biesiekierski A, Wang J, Abdel-Hady Gepreel M, Wen C. A new look at biomedical Ti-based shape memory alloys. Acta Biomater 2012;8:1661–9.

3. El-Rahman SSA. Neuropathology of aluminum toxicity in rats (glutamate and GABA impairment). Pharmacol Res. 2003;47:189–94.

4. Percy ME, Kruck TP a, Pogue AI, Lukiw WJ. Towards the prevention of potential aluminum toxic effects and an effective treatment for Alzheimer's disease. J Inorg Biochem 2011;105:1505–12.

5. Bordignon V, Palamara F, Cordiali-Fei P, Vento A, Aiello A, Picardo M, Ensoli F, Cristaudo A. Nickel, palladium and rhodium induced IFN-gamma and IL-10 production as assessed by in vitro ELISpot-analysis in contact dermatitis patients. BMC Immunol 2008;9:19.

6. Faurschou A, Menné T, Johansen JD, Thyssen JP. Metal allergen of the 21st century - A review on exposure, epidemiology and clinical manifestations of palladium allergy. Contact Dermatitis 2011;64:185–95.

7. Matsuno H, Yokoyama A, Watari F, Uo M, Kawasaki T. Biocompatibility and osteogenesis of refractory metal implants, titanium, hafnium, niobium, tantalum and rhenium. Biomaterials 2001;22:1253–62.

8. Lee J-W, Lee K-B, Jeon H-S, Park H-K. Effects of surface nano-topography on human osteoblast filopodia. Anal Sci 2011;27:369.

9. Popp J, Laflin K, Love B, Goldstein A. In vitro evaluation of osteoblastic differentiation on amorphous calcium phosphate-decorated poly(lactic-co-gylolic acid) scaffolds. J Tissue Eng Regen Med 2011;5:780–9.

10. Hynowska A, Blanquer A, Pellicer E, Fornell J, Suriñach S, MD B, Gebert A, M C, J E, Nogues C, Ibañez E, Barrios L, Sort J. Nanostructured Ti-Zr-Pd-Si- (Nb) bulk metallic composites : Novel biocompatible materials with superior mechanical strength and elastic recovery. J Biomed Mater Res Part B Appl Biomater 2014;1–11.

11. Bacakova L, Filova E, Parizek M, Ruml T, Svorcik V. Modulation of cell adhesion, proliferation and differentiation on materials designed for body implants. Biotechnol Adv 2011;29:739–67.

12. Wei J, Igarashi T, Okumori N, Igarashi T, Maetani T, Liu B, Yoshinari M. Influence of surface wettability on competitive protein adsorption and initial attachment of osteoblasts. Biomed Mater 2009;4:045002.

13. Ballester-Beltrán J, Rico P, Moratal D, Song W, Mano JF, Salmerón-Sánchez M. Role of superhydrophobicity in the biological activity of fibronectin at the cell–material interface. Soft Matter 2011;7:10803.

14. Czekanska EM, Stoddart MJ, Richards RG, Hayes JS. In search of an osteoblast cell model for in vitro research. Eur Cells Mater 2012;24:1–17.

15. Vandrovcova M, Jirka I, Novotna K, Lisa V, Frank O, Kolska Z, Stary V, Bacakova L. Interaction of Human Osteoblast-Like Saos-2 and MG-63 Cells with Thermally Oxidized Surfaces of a Titanium-Niobium Alloy. PLoS One 2014;9:100475.

16. Dowling DP, Miller IS, Ardhaoui M, Gallagher WM. Effect of Surface Wettability and Topography on the Adhesion of Osteosarcoma Cells on Plasma-modified Polystyrene. J Biomater Appl 2011;26:327–47.

17. Wang W, Poh CK. Titanium Alloys in Orthopaedics. Titan Alloy - Adv Prop Control 2013;1–20.

18. Goriainov V, Cook R, M. Latham J, G. Dunlop D, Oreffo ROC. Bone and metal: An orthopaedic perspective on osseointegration of metals. Acta Biomater 2014;10:4043–57.

19. Liskova J, Babchenko O, Varga M, Kromka A, Hadraba D, Svindrych ZdenekBurdikova Z, Bacakova L. Osteogenic cell differntation on H-terminated and O-terminated nanocrystalline diamond films. Int J Nanomedicine 2015;10:1–16.

20. Jirka I, Vandrovcova M, Frank O, Tolde Z, Plsek J, Luxbacher T, Bacakova L, Stary V. On the role of Nb-related sites of an oxidized beta-TiNb alloy surface in its interaction with osteoblast-like MG-63 cells. Mater Sci Eng C 2013;33:1636–45.

21. Kopova I, Stráský J, Harcuba P, Landa M, Janeček M, Bačákova L. Newly developed Ti–Nb–Zr–Ta–Si–Fe biomedical beta titanium alloys with increased strength and enhanced biocompatibility. Mater Sci Eng C 2016;60:230–8.

22. Foppiano S, Marshall SJ, Marshall GW, Saiz E, Tomsia AP. Bioactive glass coatings affect the behavior of osteoblast-like cells. Acta Biomater 2007;3:765–71.

23. Gittens RA, Olivares-Navarrete R, Hyzy SL, Sandhage KH, Schwartz Z, Boyan BD. Superposition of nanostructures on microrough titanium–aluminum–vanadium alloy surfaces results in an altered integrin expression profile in osteoblasts. Connect Tissue Res 2014;55:164–8.

24. Schwartz Z, Raz P, Zhao G, Barak Y, Tauber M, Yao H, Boyan BD. Effect of micrometer-scale roughness of the surface of Ti6Al4V pedicle screws in vitro and in vivo. J Bone Joint Surg Am 2008;90:2485–98.

25. Santiago-Medina P, Sundaram PA, Diffoot-Carlo N. The effects of micro arc oxidation of gamma titanium aluminide surfaces on osteoblast adhesion and differentiation. J Mater Sci Mater Med 2014;25:1577–87.

Figure captions

Figure 1. Albumin and fibronectin adsorption on the different sample surfaces measured by ELISA. PS: polystyrene. Different superscripts on top of the columns denote significant differences between groups not sharing the same superscript ($p < 0.05$).

Figure 2. Mean spreading area of Saos-2 cells after 24h in culture on alloys and controls surfaces (glass and polystyrene, PS). Different superscripts on top of the columns denote significant differences between groups not sharing the same superscript ($p < 0.05$).

Figure 3. Vinculin and actin distribution in human Saos-2 cells grown on TiZrPdSi (a) and TiZrPdSiNb (b) alloys, and on a glass coverslip (c). Stress fibres (red), focal contacts (green) and nuclei (blue) can be observed. Fluorescence intensity of vinculin signal normalized to the total amount of pixels evaluated (d). Different superscripts on top of the columns denote significant differences between groups not sharing the same superscript ($p < 0.05$).

Figure 4. Proliferation of Saos-2 cells grown on TiZrPdSi and TiZrPdSiNb alloys, and on glass coverslip and polystyrene (PS) surfaces at 1, 3 and 7 days in culture.

Figure 5. Quantification of mRNA levels. Relative expression of Osteocalcin (OC), Osteopontin (OPN), Osteonectin (ON) and Bone sialoprotein II (BSP) in Saos-2 cells on day 7 and 14 after seeding on TiZrPdSi and TiZrPdSiNb alloys, and on a glass coverslip. The target gene levels are expressed as a relative value, i.e. the ratio of the target gene expression toward the reference *GAPDH* gene. Different superscripts on top of the columns denote significant differences ($p < 0.05$) among the materials at the same time-point.

Figure 6. Fluorescence intensity of COLI (a), OC (b) and ALP (c) osteoblast differentiation proteins in Saos-2 cells grown on TiZrPdSi, TiZrPdSiNb and glass surfaces for 7 days. Different superscripts on top of the columns denote significant differences between groups not sharing the same superscript ($p < 0.05$).

Figure 7. ALP activity of Saos-2 cells grown on TiZrPdSi alloy, TiZrPdSiNb alloy and glass coverslip after 7 and 14 days in culture. Values are normalized with total protein content. Different superscripts on top of the columns denote significant differences between groups not sharing the same superscript ($p < 0.05$).

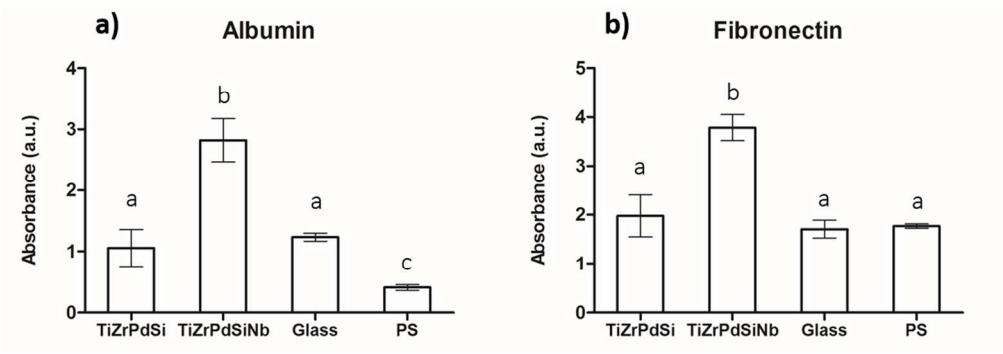

Figure 1. Albumin and fibronectin adsorption on the different sample surfaces measured by ELISA. PS: polystyrene. Different superscripts on top of the columns denote significant differences between groups not sharing the same superscript ($p < 0.05$).

73x25mm (600 x 600 DPI)

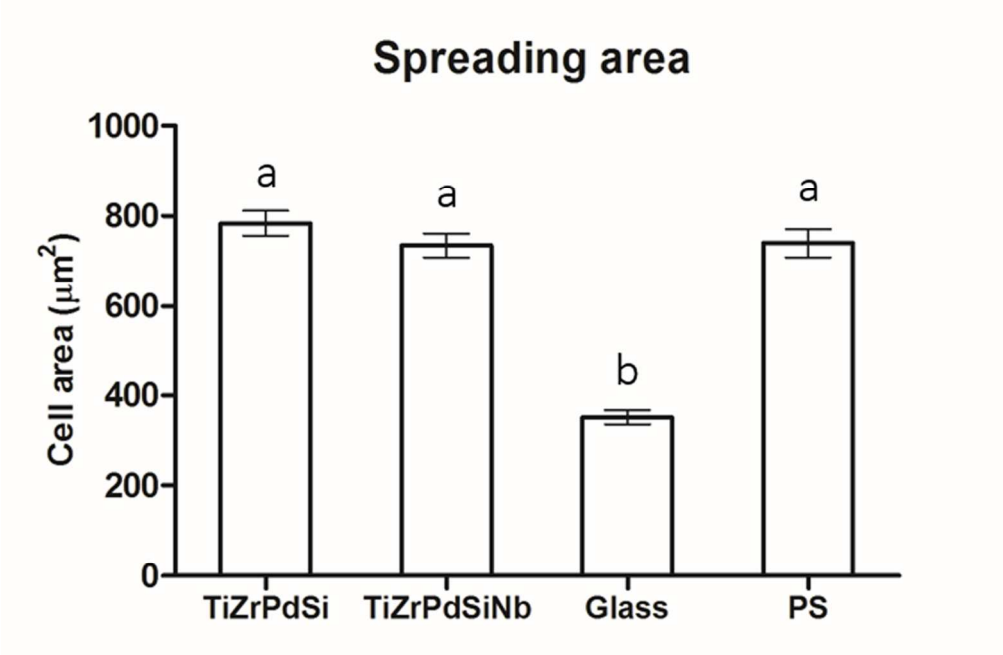

Figure 2. Mean spreading area of Saos-2 cells after 24h in culture on alloys and controls surfaces (glass and polystyrene, PS). Different superscripts on top of the columns denote significant differences between groups not sharing the same superscript ($p < 0.05$).

73x48mm (600 x 600 DPI)

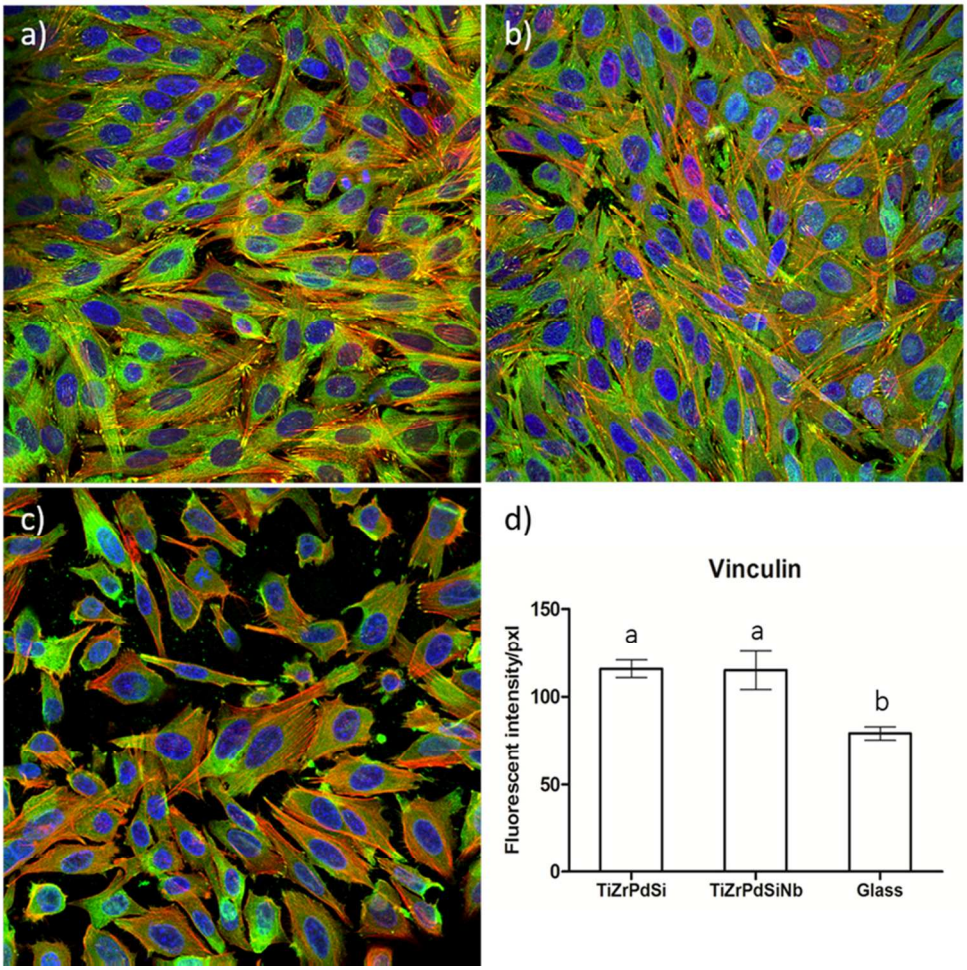

Figure 3. Vinculin and actin distribution in human Saos-2 cells grown on TiZrPdSi (a) and TiZrPdSiNb (b) alloys, and on a glass coverslip (c). Stress fibres (red), focal contacts (green) and nuclei (blue) can be observed. Fluorescence intensity of vinculin signal normalized to the total amount of pixels evaluated (d). Different superscripts on top of the columns denote significant differences between groups not sharing the same superscript ($p < 0.05$).

87x84mm (300 x 300 DPI)

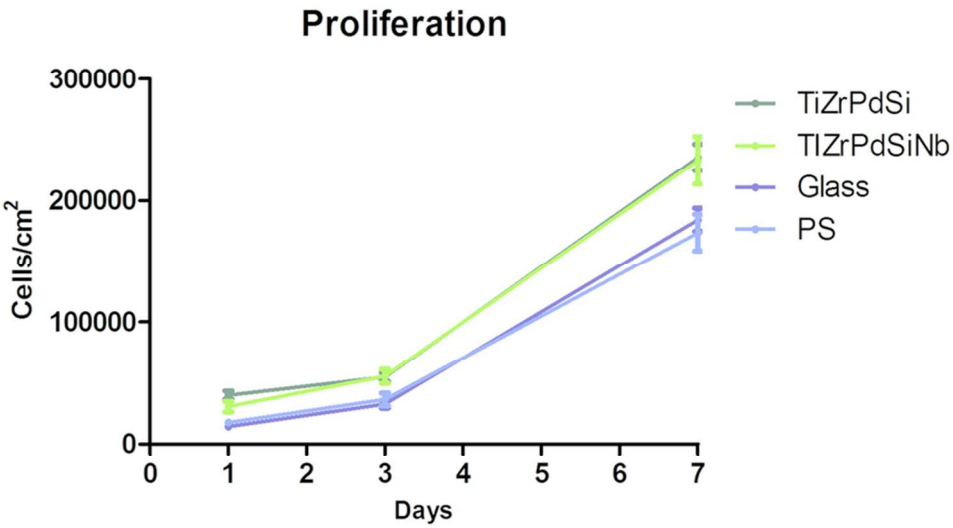

Figure 4. Proliferation of Saos-2 cells grown on TiZrPdSi and TiZrPdSiNb alloys, and on glass coverslip and polystyrene (PS) surfaces at 1, 3 and 7 days in culture.

79x45mm (300 x 300 DPI)

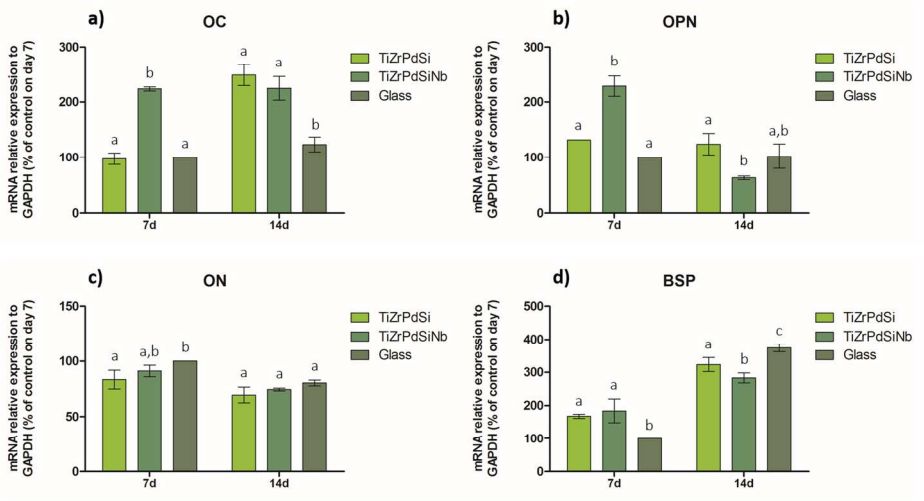

Figure 5. Quantification of mRNA levels. Relative expression of Osteocalcin (OC), Osteopontin (OPN), Osteonectin (ON) and Bone sialoprotein II (BSP) in Saos-2 cells on day 7 and 14 after seeding on TiZrPdSi and TiZrPdSiNb alloys, and on a glass coverslip. The target gene levels are expressed as a relative value, i.e. the ratio of the target gene expression toward the reference GAPDH gene. Different superscripts on top of the columns denote significant differences ($p < 0.05$) among the materials at the same time-point.

171x95mm (300 x 300 DPI)

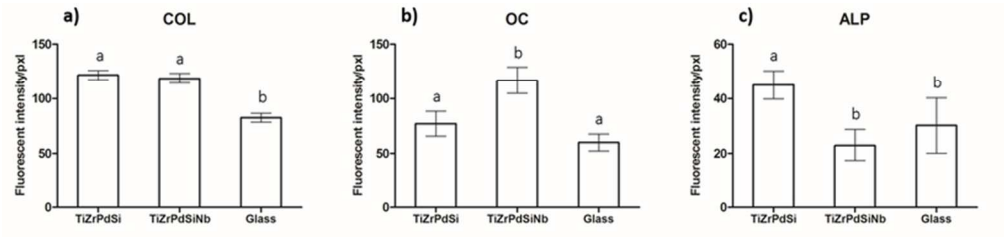

Figure 6. Fluorescence intensity of COLI (a), OC (b) and ALP (c) osteoblast differentiation proteins in Saos-2 cells grown on TiZrPdSi, TiZrPdSiNb and glass surfaces for 7 days. Different superscripts on top of the columns denote significant differences between groups not sharing the same superscript ($p < 0.05$).

34x8mm (600 x 600 DPI)

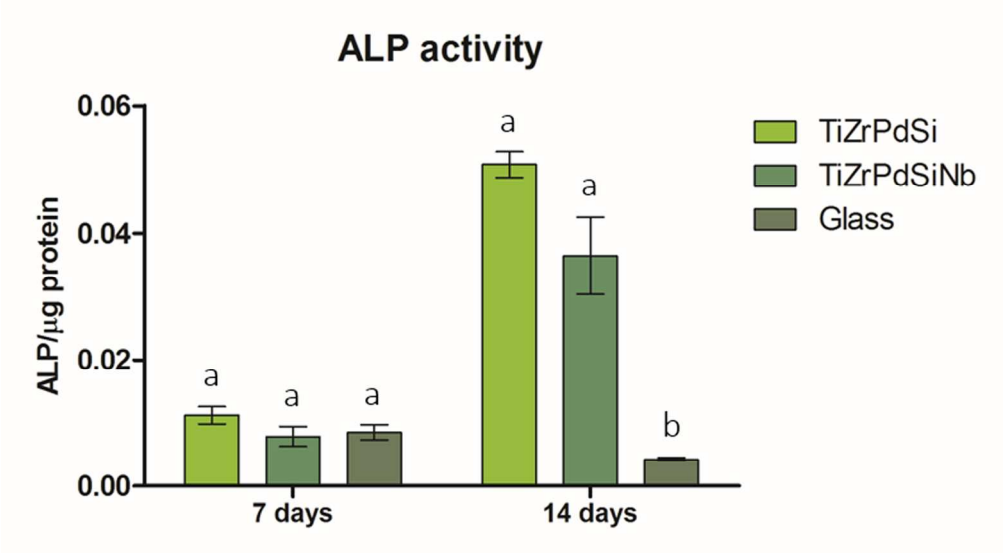

Figure 7. ALP activity of Saos-2 cells grown on TiZrPdSi alloy, TiZrPdSiNb alloy and glass coverslip after 7 and 14 days in culture. Values are normalized with total protein content. Different superscripts on top of the columns denote significant differences between groups not sharing the same superscript ($p < 0.05$).

140x77mm (300 x 300 DPI)